

Optimization of Iron Oxide Nanoparticles Detection using Ultrashort TE Imaging

O. M. Girard¹, K. N. Sugahara², L. Agemy², E. Ruoslahti², G. M. Bydder¹, and R. F. Mattrey¹

¹Department of Radiology, University of California, San Diego, CA, United States, ²Vascular Mapping Center, Burham Institute for Medical Reserach at UCSB, Santa Barbara, CA, United States

Purpose: Iron oxide nanoparticles (IONPs) have been used in various Magnetic Resonance Imaging (MRI) applications [1], mostly as negative contrast agents. Their strong magnetic moment causes signal dephasing that results in signal void on T_2^* -weighted images obtained at a long echo time (TE). A major challenge when using IONPs is the need to recognize regions of signal void due to IONPs from low-signal tissues or susceptibility artifacts, particularly when the signal-to-noise ratio is low. While a pre-contrast image can help, the slow accumulation of IONP in tissues makes co-localization challenging. Several investigators have recently developed acquisition strategies to generate positive contrast from IONPs [2-4]. A common feature of those approaches is that they all rely on the magnetic field perturbations caused by IONP that share a similar origin to the T_2^* -effect. IONPs also have intrinsic T_1 shortening properties [5] that may lead to positive contrast using appropriate sequences. Relying on this effect to generate a positive contrast should increase the detection specificity of IONPs since a different mechanism is involved. We have previously reported the potential of ultrashort TE (UTE) imaging [6] to generate a positive contrast from IONP even at relatively high concentration [7]. Here we focus on the optimization of UTE acquisition strategies for IONPs. Both T_2^* and T_1 effects are analyzed and synergistic T_1 - T_2^* positive contrast that relies on an appropriate UTE imaging subtraction scheme is also described.

Materials and methods: Theory and Simulation: The usual spoiled gradient echo (SPGR) signal equation was used to model MRI signal (S) as a function of TE, repetition time (TR) and flip angle (FA). TE was arbitrarily set to zero in order to simulate the UTE signal. The subtraction of a later echo signal from the UTE signal (i.e. $S(UTE) - S(TE)$) was also studied, leading to a composite image (SubUTE) that provides hybrid contrast different from the usual T_1 and T_2^* contrast. A linear dependency of relaxation rates as a function of IONP concentration was assumed allowing the use of constant relaxivities r_1 and r_2^* . We investigated the contrast arising from a given amount of IONP from a background tissue defined by the unenhanced relaxation times T_{10} and T_{20}^* . Contrast-to-noise ratio (CNR) was calculated for SPGR (including UTE) and SubUTE signals, and optimized as a function of MR imaging parameters. A $\sqrt{2}$ noise amplification was considered for SubUTE, corresponding to the summation of uncorrelated noise of the same intensity from the 2 original images. A short TR was considered ($\leq T_1$) since it corresponds to the optimal contrast efficiency regime for both T_1 - and T_2^* - weighted gradient echo sequences, as long as it is possible to adjust the FA to preserve optimal contrast [8]. **In Vitro Experiments:** IONP nanoworms [9] (about 80×10 nm elongated-shape particles) were characterized by MRI. Several concentrations were prepared (0, 0.09, 0.18, 0.9 and 1.8 mM Fe), by diluting the IONPs in a 1.8% agarose gel. T_1 , T_2^* and the corresponding relaxivities were measured with inversion-recovery fast spin echo (FSE) and multi-echo gradient echo sequences respectively. Several multiecho-UTE acquisitions were run with varying TEs (from 8µs to 33ms) and FAs (10, 30, 50 and 70°) while keeping TR fixed at 300ms. **In Vivo Experiments:** Tumor-bearing mice with orthotopically implanted prostate cancer were imaged before and ~7 hours after injection of 5 mg iron per kg of a tumor-targeted form of the nanoworms [10]. Mice were scanned using a 2.5cm bird-cage coil at 3T starting with a T_2 -weighted FSE (TR/TE=6.4s/70ms) followed by a multiecho (8.10⁻³, 6.2, 11.4 and 16.5 ms nominal TEs) UTE sequence (TR=90ms, FA=50°). All experiments were performed on a 3T Signa TwinSpeed scanner (GE Healthcare, WI, USA) at room temperature. The simulation was implemented with Mathematica (Wolfram Research Inc., IL, USA).

Results and Discussion: Measured T_1 and T_2^* relaxivities were $r_1 \approx 4.5$ and $r_2^* \approx 145 \text{ mM}^{-1} \cdot \text{s}^{-1}$. Figure 1 displays a comparison between experiments and theory for a 50° FA, using the measured relaxivities and baseline relaxation times ($T_{10}=2.7\text{s}$ and $T_{20}^*=25\text{ms}$ for the 1.8% agarose gel). The data shows that the T_1 contrast is stronger than the T_2^* contrast for the studied IONPs and "tissue" in our experimental condition (2mm slice thickness). The agreement is very good although the curves do not exactly fit, especially for high concentrations. This could be attributed to artifacts, non-zero actual UTE or limitations in our model. Figure 2 shows theoretical graphs that compare T_1 -, T_2^* -, and synergistic T_1 - T_2^* -contrast, for two different sets of baseline relaxation times and the measured relaxivities, using a 0.1mM IONP concentration. Isocontours were calculated in reference to the maximal achievable contrast (indicated by the 99% line) for a given tissue and IONP concentration. For the regular SPGR sequence it shows (especially in b) that the contrast is positive (T_1 effect) at ultrashort TE and progressively becomes negative (predominant T_2^* effect) as TE is lengthened. Conversely the SubUTE signal provides a single positive-contrast regime (hybrid contrast). A high T_{10}/T_{20}^* ratio (a) similar to the experimental conditions of Fig. 1) is highly favorable for T_1 contrast while a moderate ratio (one order of magnitude in b) provides more balanced T_1 and T_2 contrasts. In the latter case the SubUTE strategy provides optimal contrast. Similar results were obtained over a wide range of IONP concentrations (nM to 10s of mM). Representative *in vivo* results are displayed in Figure 3. They illustrate clearly the potential of positive-contrast strategies using UTE sequences.

Conclusion: Our results show that, contrary to conventional wisdom, T_1 -contrast can be superior to T_2^* -contrast when imaging with IONPs. This is explained by the fact that despite the high r_2^*/r_1 ratio of IONPs, the actual T_1 and T_2^* variations induced by IONPs are strongly influenced by the baseline tissue relaxation times. Hence a high T_{10}/T_{20}^* ratio can counterbalance the stronger r_2^* effect of IONP and make the T_1 effect dominant. Interestingly, when T_1 and T_2^* -contrast intensities are similar, the SubUTE image leads to the optimal detection of IONP, because it combines the two effects in a synergistic way. In addition, UTE and SubUTE sequences reduce ambiguity compared to non-subtracted long echo images since all regions containing IONPs appear hyperintense, no matter how high the concentration (see Fig. 1). A multiecho UTE sequence can then be used very efficiently to generate three different types of contrast in a single acquisition, providing increased detection sensitivity and specificity while benefiting from positive contrast.

Figure 2: CNR as a function of TE and FA. TR=300ms, [IONP]=0.1mM, $r_1=4.5 \text{ mM}^{-1} \cdot \text{s}^{-1}$, $r_2^*=145 \text{ mM}^{-1} \cdot \text{s}^{-1}$

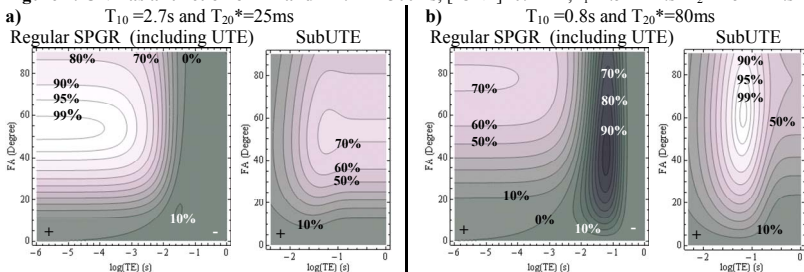


Fig.1: Experimental (top row) VS Simulated (bottom row) MR signal as a function of TE. Left: regular SPGR signal, including UTE. Right: SubUTE

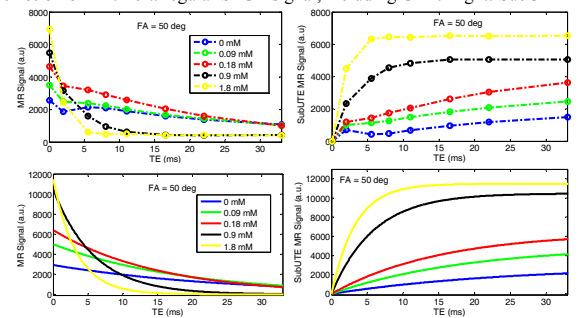
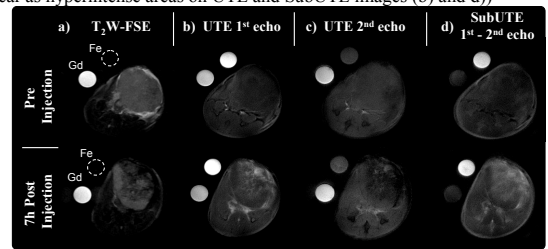


Figure 3: In Vivo Results. Axial images of a tumor bearing mouse. Post-injection, IONPs produce signal voids on T_2^* -weighted images (a) and (c) but appear as hyperintense areas on UTE and SubUTE images (b) and (d))



Acknowledgments: This work was supported in part by the NIH ICMIC P50-CA128346, CCNE U54-CA119335, and Pfizer.

References: [1] Corot, C, et al., *Adv Drug Deliver Rev*, 2006; 58(14): p. 1471 [2] Cunningham, CH, et al., *Magn Reson Med*, 2005; 53(5): p. 999 [3] Liu, W, et al., *NMR Biomed*, 2008; 21(3): p. 242-250 [4] Mani, V, et al., *Magn Reson Med*, 2006; 55(1): p. 126 [5] Roch, A, et al., *J Chem Phys*, 1999; 110(11): p. 5403 [6] Robson, MD, et al., *J Comput Assist Tomo*, 2003; 27(6): p. 825 [7] Girard, OM, et al., *Proc. ISMRM 17*, 2009: p. 2769 [8] Busse, RF, *Magn Reson Med*, 2005; 53(4): p. 977 [9] Park, JH, et al., *Adv Mater*, 2008; 20(9): p. 1630 [10] Agemy, L, et al., *Proc. AACR 100*, 2009: p.335.